STIINTE 07, Sinaia

Stein Haaland, Max-Planck Institute,/ University of Bergen
Goetz Paschmann, Max-Planck Institute

31 May 2007

Contents

— 1 —

Minimum Variance Analysis

In the following, we outline the theory behind minimum variance analysis of the magnetic field (MVAB) and present a step-by-step example using Cluster data. The theory section is partly based on Sonnerup and Scheible (1998).

1.1 Theory

In this context, the main purpose of minimum variance analysis (MVA) is to find an estimate of the orientation of a nearly one-dimensional discontinuity such as acurrent sheet or wave front. In Figure 1.1, this means that we have to find the unit vectors of the yet unknown coordinate system xyz. The orientation of the discontinuity is uniquely described by its normal, i.e., the unit vector along $\mathbf{z}$.

Concider first the ideal one-dimensional discontinuity in Figure 1.1a). For this case, the expression of divergence can be expressed

$$\nabla \cdot \mathbf{B} = \frac{\partial B_z}{\partial z} = 0 \tag{1.1}$$

Similarly, Faraday's law reduces to

$$\nabla \times \mathbf{E} = -\frac{\partial B}{\partial t} = -\frac{\partial B_z}{\partial t} \tag{1.2}$$

The magnetic field along the z-direction, which is the sought after estamate of the normal direction, thus have *no variance*, either temporal or spatial.

For real cases, as illustrated in Figure 1.1b), there will alost always be deviation from this simple model, either due to internal structures in the discontinuity, or due to time variations. In practice, one therefore has to find the direction with *minimum variance* in the magnetic field. For a case with N discrete measurmenets, this implies a minimization of the following residue

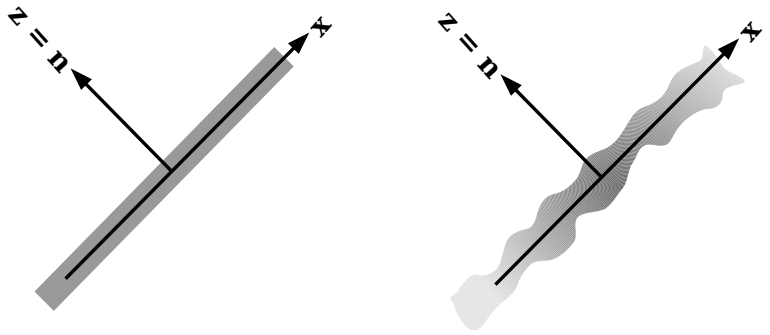

Figure 1.1: *Left : ideal 1-D discontinuity. Right : realistic nearly 1-D discontinuity. The sought-after orientation is described by the normal vector,* $\mathbf{n}$.

$$\sigma^2 = \frac{1}{N}\sum_{i=1}^{N} \left|(\mathbf{B}^{(i)} - \langle \mathbf{B} \rangle) \cdot \hat{\mathbf{n}}\right|^2 \tag{1.3}$$

where N is the number of samples, $\mathbf{B}^{(i)}$ means sample number i, and the brackets $\langle\ \rangle$ denote an ensemble average.

Differention with respect to $\mathbf{n} = [n_x, n_y, n_z]$ yields three linear equations

$$\begin{aligned} &\frac{\partial}{\partial n_x}\left(\sigma^2 - \lambda(|\hat{\mathbf{n}}|^2 - 1)\right) \\ &\frac{\partial}{\partial n_y}\left(\sigma^2 - \lambda(|\hat{\mathbf{n}}|^2 - 1)\right) \\ &\frac{\partial}{\partial n_z}\left(\sigma^2 - \lambda(|\hat{\mathbf{n}}|^2 - 1)\right) \end{aligned} \tag{1.4}$$

where λ is a so-called Lagrange multiplier (which here describe the actual variance along each direction) used to impose the constraint $|\mathbf{n}| = 1$.

After differentiation, these three equations can be written on matrix form :

$$\sum_{i=1}^{3} \left(\langle B_i B_j \rangle - \langle B_i \rangle \langle B_j \rangle\right) n_j = \lambda n_i \tag{1.5}$$

It is seen that the λ values are eigenvalues, and n_i are eigenvectors of the covariance matrix Q = $\langle B_i Bj \rangle - \langle B_i \rangle \langle B_j \rangle$.

Minimum variance analysis of the magnetic field thus consist of finding the eigenvalues and eigenvectors of the covariance matrix Q. The eigenvector corresponding to the lowest eigenvalue (= minimum variance) is an estimate of the normal direction of the discontinuity.

The ratio between the eigenvalue indicate how well the components of the new coordinate system are resolved. Three distinct eigenvalues ($\lambda_1 \ll \lambda_2 \ll \lambda_3$) are desirable, but not always achieved. The ratio λ_2/λ_1 is often used as a quality estimate of MVA, but a large eigenvalue ratio does not necessarily mean a correct normal estimation.

1.2 Step-by-step example

In order to illustrate step-by-step how MVAB can be applied to fin a boundary normal, we will use data from the Cluster C2 spacecraft during a magnetopause crossing on 5 July, 2001. This event has been described in detail by Haaland et al. (2004), and also carefully examined by Hasegawa et al. (2004) who reconstructed the topology, and by Sonnerup et al. (2004) who used is as a bechmark data. The data are given in a GSE coordinate system, so eigenvectors and the orientation of the discontinuity will also be expressed in GSE coordinates.

Figure 1.2 shows an overview of the magnetic field for this event. We will use 17 samples of magnetic field data from Cluster C2 (red line) for the time interval 06:23:20 to 06:24:25 to illustrate the use of MVA.

The 17 individual B-field vectors, here presented as a 3x17 matrix in a GSE coordinate system and truncated to two digits, are:

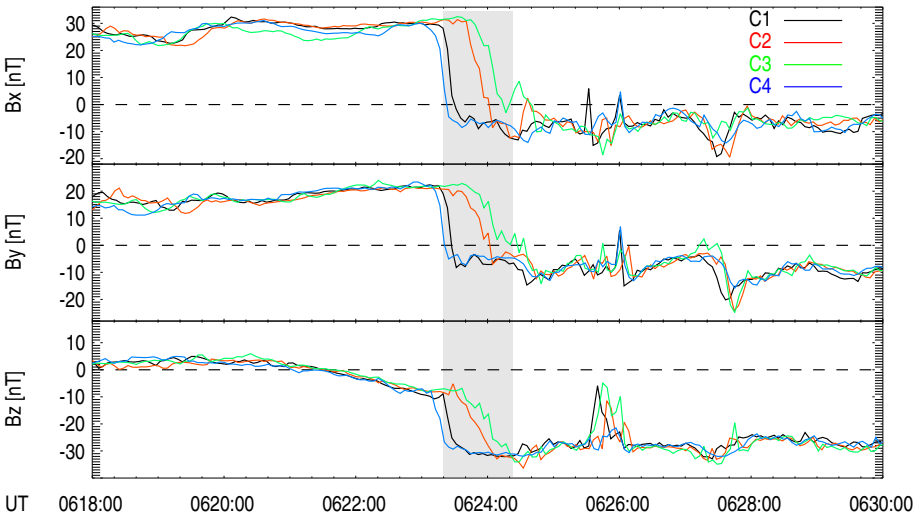

Figure 1.2: *Magnetic field during a Cluster magnetopause crossing on 5 July 2005. Data from C2 (red line) during the shaded time interval will used to illustrate minimum variance.*

$$\mathrm{B}' = \begin{bmatrix} 31.41 & 20.72 & -8.49 \\ 31.18 & 20.62 & -9.21 \\ 29.76 & 18.33 & -5.18 \\ 31.41 & 20.12 & -9.70 \\ 30.55 & 19.86 & -11.89 \\ 30.89 & 17.93 & -13.06 \\ 22.23 & 13.83 & -17.54 \\ 16.29 & 12.65 & -19.42 \\ 13.35 & 9.92 & -21.65 \\ 2.66 & 2.30 & -25.19 \\ 2.38 & 4.52 & -28.04 \\ -8.57 & -7.00 & -30.60 \\ -6.13 & -5.43 & -32.90 \\ -6.97 & -4.44 & -31.55 \\ -6.98 & -2.46 & -32.04 \\ -12.34 & -3.16 & -32.31 \\ -11.60 & -4.38 & -32.75 \end{bmatrix} \tag{1.6}$$

1.2.1 Step 1 - removing the sample mean

It is convenient to remove the sample means from of the input variables in the data matrices. Most of the methods we will introduce in this chapter assume zero mean or automatically removes the mean. There is no loss of generality in doing this, as the variance of a time series does not cange by adding a constant. The sample mean of our magnetic field, b_{cj} is simply the mean of the individual columns in our data matrix B':

$$\overline{b_{cj}} = \frac{1}{N} \sum_{j=1}^{N} b_{ij} \tag{1.7}$$

The means of each column in our data matrix B', i.e., the means of B'_x, B'_x and B'_x are:

$$\langle \mu \rangle = \begin{bmatrix} 11.1475 & 7.8791 & -21.2701 \end{bmatrix} \tag{1.8}$$

and the resulting matrix B with the sample mean removed becomes:

$$\mathrm{B} = \begin{bmatrix} 20.258 & 12.842 & 12.778 \\ 20.030 & 12.743 & 12.058 \\ 18.616 & 10.456 & 16.095 \\ 20.267 & 12.243 & 11.570 \\ 19.403 & 11.985 & 9.371 \\ 19.749 & 10.058 & 8.206 \\ 11.088 & 5.956 & 3.723 \\ 5.151 & 4.778 & 1.845 \\ 2.206 & 2.042 & -0.380 \\ -8.479 & -5.574 & -3.928 \\ -8.766 & -3.353 & -6.778 \\ -19.724 & -14.881 & -9.333 \\ -17.284 & -13.317 & -11.635 \\ -18.126 & -12.328 & -10.289 \\ -18.135 & -10.346 & -10.778 \\ -23.495 & -11.044 & -11.045 \\ -22.756 & -12.263 & -11.481 \end{bmatrix} \tag{1.9}$$

1.2.2 Step 2 - obtaining the covariance matrix

Th covariance between two time series or data sets (with zero mean) is defined as

$$q_{ij} = \frac{1}{N} \sum_{k=1}^{N} x_{ki} x_{kj} \tag{1.10}$$

which is equivalent to

$$\mathsf{Q} = \mathsf{B}^T \mathsf{B}/N \tag{1.11}$$

where N is the number of observations (here 17) and the superscript ^{T} means transpose. The covariance matrix $\mathrm{Q} = \langle B_i Bj \rangle - \langle B_i \rangle \langle B_j \rangle$, thus becomes :

$$\mathbf{Q} = \begin{bmatrix} 297.269 & 178.502 & 165.233 \\ 178.502 & 109.784 & 99.550 \\ 165.233 & 99.550 & 96.109 \end{bmatrix} \tag{1.12}$$

1.2.3 Step 2 - eigenvalues and eigenvectors

With the covariance matrix known, we can now compute the eigenvalues, λ_i by solving the characteristic equation :

$$|\mathrm{Q} - \lambda \mathrm{I}| = 0 \tag{1.13}$$

where I is the identity matrix. The resulting eigenvalues, listed in decreasing order are $\lambda_1 = 497.79$, $\lambda_2 = 3.50$ and $\lambda_3 = 1.87$. The corresponding eigenvectors, are the rows of the matrix

$$\mathbf{A} = \begin{bmatrix} -0.77161 & -0.46605 & -0.43291 \\ 0.29021 & 0.34768 & -0.89157 \\ 0.56603 & -0.81358 & -0.13302 \end{bmatrix} \tag{1.14}$$

In the above matrix, the eigenvectors are orthonormal, i.e., perpendicular to each other, and normalized so that $|\mathbf{a_i}| = 1$. The eigenvector associated with the smallest eigenvalue gives an estimate of the boundary normal, $\mathbf{n} = [0.56603, -0.81358, -0.13302]$, of the magnetopause, while the other two eigenvectors define the tangential plane of the magnetopause. The eigenvalue ratio serve as a measure of the uncertainty in the direction of the eigenvectors (Sonnerup and Scheible, 1998).

For any eigenvalue problem like the one in Equation (1.13), the sense of the first eigenvector is undetermined and can be chosen by the user (or by the software package used !). The direction of the eigenvector is therefore arbitrary, and different software packages may therfore return different signs of the eigenvectors.

Step 3 - principal components

The eigenvector matrix (Equation 1.14) can now be used to rotate the original data set into a new, orthogonal *principal component* coordinate system.

$$\mathsf{Y} = \mathsf{BA} \tag{1.15}$$

In the resulting matrix, Y, has the same units and average as the original input matrix B, but three components are sorted now after variance. Since the largest eigenvalue was significantly larger than the intermediate and minimum eigenvalues, most of the variance and thus information of the magnetic field is now collected in one component. This is often the case for nearly one-dimensional discontinuities, and will be utilized in the next chapter.

1.3 Adding Q-matrices

So far, only measurements from one spacecraft were used. If one assumes that the all four spacecraft traverses the same discontinuity, it is possible to combine information from two or more spacecraft. This is done by adding a set of suitable weighted and normalized covariance matrices from each spacecraft, and then calculate the eigenvalues and eigenvectors of the combined matrix. The weighting and normalization of the individual Q-matrix is not unique, but it is desireable to put more emphasis on results where the eigenvalues are well separated, for example by multiplying each individual covariance matrix with the before mentioned eigenvalue ratio; $w^{(k)} = \lambda_2^{(k)}/\lambda_1^{(k)}$, where the index k denotes the spacecraft.

A composite matrix with weights, w_k for each method, can thus be expressed

$$Q_{COM_{ij}} = \sum_{k=1}^{k=K} w^{(k)} Q_{ij}^{(k)} \tag{1.16}$$

As with a single Q-matrix, the composite normal of the discontinuity is now given by the composite eigenvector corresponding to the smallest eigenvalue.

Similarly, it is also possible to combine different methods, e.g. MVAB and other variance methods (see e.g. Sonnerup et al., 2004; Sonnerup et al., 2006; Haaland et al., 2006).

1.4 Exercises

Datasets for the exercises are available on *www.issi.unibe.ch/~haaland/Sinaia07/* (or given alternative URL).

1) Do a minimum variance analysis of the magnetic field data from Cluster SC2 from 5 July 2001. What is the orientation of the boundary normal ?

2) Swap the first and last record and redo the the analysis. What happens to the variance analysis?

2) Remove the first and last sample of the data matrix (Equation 1.6), and redo the analysis.

3) Do a deHoffmann-Teller analysis of the data. What is the velocity of the boundary along the normal? Is there any difference between the data from Spacecraft SC1 and SC3?

4) Construct a Walen plot of the datasets from SC1 and SC2 (tip : calculate the Alfven velocity, VA, plot this component by component versus the quantity (VHT - V)). Is there any difference between SC1 and SC2 ?

5) Fetch the magnetic field data from all four spacecraft, do a minimum variance analysis of each spacecraft for the time interval 06:23:00 - 06:24:40. Thereafter, combine the matrices as described in Section 1.3. What is the composite normal ?

— 2 —

Multispacecraft Discontinuity Analysis

In this chapter we present a simple method to derive orientation and speed of a discontinuity from simultaneous measurements of a field or plasma quantity from four spacecraft.

2.1 Theory

Four spacecraft timing methods utilize the fact that a single common feature of a discontinuity can be identified at four different locations at different (or sometimes simultaneous) times when crossing the discontinuity. Identifying the common feature and timetagging this at each of the four spacecraft is therefore an essential element of timing methods. Additional information, for example the duration of a crossing can give valuable information about any evolution or acceleration of the discontinuity.

2.1.1 Crossing times and duration

Crossing times and durations can in principle be derived from any measured quantity provided that the time resolution is sufficient. Experience with Cluster suggest that the magnetic field or density proxies from the EFW instruments provide the best results. Timing and duration from the magnetic field are often easier to estimate if the measurements are rotated into a maximum variance coordinate system. A common coordinate system for all four spacecraft may be used (see Section 1.3), but this is not critical since the direction of the maximum variance component is typically well determined.

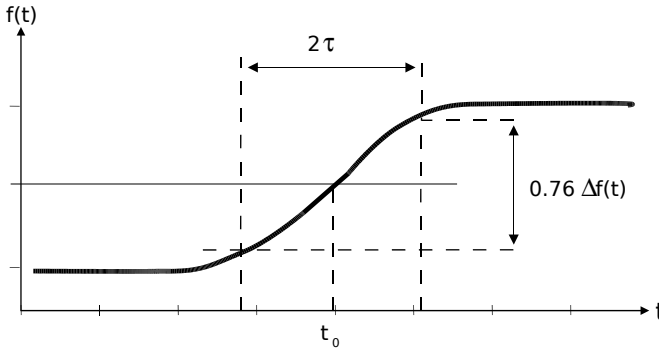

Figure 2.1: *Idealized magnetic field (or density) profile across a discontinuity, and one possible definition of crossing time, t_0, and crossing duration, $2\,\tau$. With a known velocity, $V_d(t)$, of the discontinuity, the thickness, d_d is given by $2\tau * \mathrm{V_{MP}(t)}$. After Paschmann et al. (2005)*

For many discontinuities, the maximum variance component, B_{max} of the magnetic field resemble a Harris sheet like profile; $B_{max}(t) = f(t) \propto tanh(t/2\,\tau)$ (see e.g., Haaland et al., 2004; Paschmann et al., 2005; Thompson et al., 2005). For such cases, a natural definition of crossing time, denoted t_0 in Figure 2.1, is the time where $f(t)$ has reached 50% of its extremal value. Also, the hyperbolic tangent curve representing a Harris sheet has the property that 76% of the total change, $\Delta f(t)$ occurs within the characteristic time interval $2\,\tau$.

Crossing times, t_c (c=0,1,2,3), for each crossing is here defined as the time where measured quantity f(t) crosses the zero line. This definition of crossing time is not unique; as the multi-spacecraft methods rely on relative timing only, any distinct feature observed by all spacecraft can be used for timing.

2.1.2 Velocity and orientation

With relative spacecraft separation vectors, $\mathbf{r_i}$, and crossing times known, the boundary normal, $\mathbf{n}$ and velocity along this normal, $\mathbf{V_n}$, can be found from :

$$(\mathbf{V}(t_i - t_0)) \cdot \mathbf{n} = (\mathbf{r_i} - \mathbf{r_0}) \cdot \mathbf{n} \tag{2.1}$$

Given four spacecraft, the velocity and normal can thus be solved from

$$\begin{bmatrix} \mathbf{r_1} - \mathbf{r_0} \\ \mathbf{r_2} - \mathbf{r_0} \\ \mathbf{r_3} - \mathbf{r_0} \end{bmatrix} \cdot \frac{1}{\mathbf{V_n}} \begin{bmatrix} n_x \\ n_y \\ n_z \end{bmatrix} = \begin{bmatrix} t_1 - t_0 \\ t_2 - t_0 \\ t_3 - t_0 \end{bmatrix} \tag{2.2}$$

Which can be solved for $\hat{\mathbf{n}}/V_n$, e.g., by multiplying from left with the inverted separation distance matrix.

In the above method, the velocity of the discontinuity is assumed to be constant and equal at all four spacecraft. Differences in crossing duration between the spacecraft are attributed to different thicknesses. Variants of the above method which take non-constant motion into account have been presented by Haaland et al. (2004) and Paschmann et al. (2005).

2.1.3 Classification

Discontinuities are often classified as a tangential discontinuity (TD) or rotational discontinuities (RD). The difference is illustrated in Figure 2.2.

A tangential discontinuity separate two different plasma regions. There is no mixing of the two plasma regimes, and they may even have two different compositions. A TD is thus classified by zero plasma flow across (ignoring diffusion, there is no flow component along the normal), zero normal magnetic field component, and constant total pressure, $p = p_B + p_p$ across the discontinuity.

A rotational discontinuity (RD), on the other hand, may have a finite normal component, but since RDs are Alfvenic, the magnetic field changes should be correlated with changes in the plasma flow.

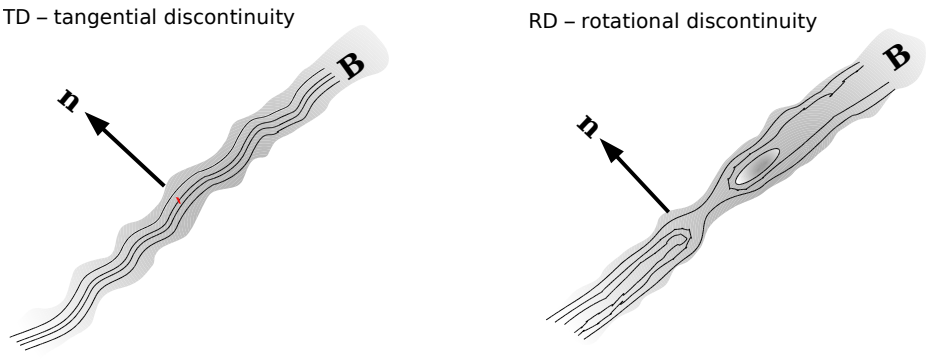

Figure 2.2: *Left: Example of a tangential discontinuity (TD). There is no magnetic field along the normal component, nor any plasma transport across the discontinuity. Right: Illustration of a rotational discontinuity (RD). There is a finite magnetic field component along the normal and plasma flow acros the boundary.*

There have been attempts to classify solar wind discontinuities as RDs or TDs based on the magnetic field alone (see e.g., Knetter et al., 2004, and references therein), but the success of such methods inherently depend on the ability to establish the true normal of the discontinuity, and there are ambiguous cases where no classifications can be done. Still, if a reliable normal has been established, a significant normal magnetic field component may indicate a rotational discontinuity and the presence of reconnection. Signatures of reconnection, e.g., plasma acceleration may provide further support for reconnection.

A more reliable method, which utilizes plasma data, is the so-called Walén test (e.g., Sonnerup et al., 1995; Khrabrov and Sonnerup, 1998). This consists of plotting the plasma bulk velocity components measured during a discontinuity crossing (after tansformation into a suitable frame, co-moving with the discontinuity - typically the deHoffmann-Teller (HT) frame), against the corresponding components of the measured Alfvén velocities. The results are characterized in terms of the slope, α and correlation coefficients between $(\mathbf{V} - \mathbf{V_{HT}})$ and $\mathbf{V_A}$. A poor correlation or slopes close to 0 indicate tangential discontinuity, whereas RDs should ideally have a slope close to 1.

2.2 Example

As a step-by-step example, we will use the same set of measurements as in the previous chapter. Figure 1.2 shows the maximum variance component of the magnetic field for this event.

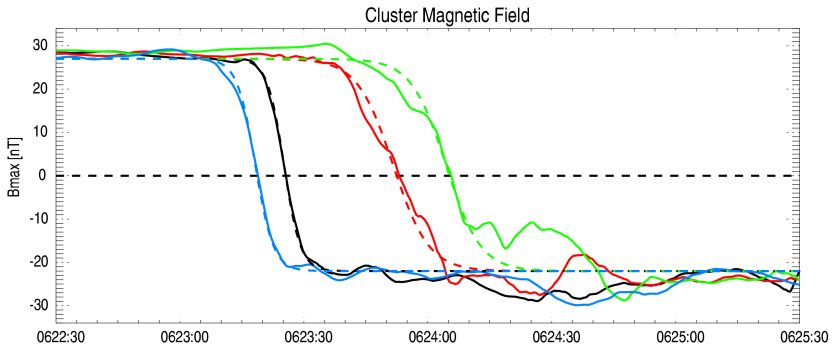

Figure 2.3: *Maximum variance component of the data set from Figure 1.2. The dashed lines show the corresponding Harris sheet fit results.*

Spacecraft positions are found in the Cluster auxillary data, and are normally available at one record per minute. The crossing used for this example, takes place around 06:23 UT and the separation distances (in km GSE) relative to spacecraft C4 (separation distance $\mathbf{r_0}$) are :

$$\begin{array}{rcl} \mathbf{r_1} - \mathbf{r_0} = & [& 1669.3 \quad 1621.7 \quad 1280.4 \quad] \\ \mathbf{r_2} - \mathbf{r_0} = & [& -387.4 \quad 1579.3 \quad 1224.1 \quad] \\ \mathbf{r_3} - \mathbf{r_0} = & [& 724.7 \quad 2513.4 \quad -400.6 \quad] \end{array} \tag{2.3}$$

Examination of Figure 2.3 shows that the spacecraft C1, C2 and C3 crosses 6.7, 33.5 and 44.4 seconds, respectively, after spacecraft C4. Inserted into Equation 2.4, we get :

$$\frac{1}{\mathbf{V_n}} \begin{bmatrix} n_x \\ n_y \\ n_z \end{bmatrix} = \begin{bmatrix} 1669.3 & 1621.7 & 1280.4 \\ -387.4 & 1579.3 & 1224.1 \\ 724.7 & 2513.4 & -400.6 \end{bmatrix}^{-1} \begin{bmatrix} 6.7 \\ 33.5 \\ 44.4 \end{bmatrix} \tag{2.4}$$

Which gives a normal $\mathbf{n} = [-0.53208, 0.83282, -0.15265]$ and a velocity $V_n = 39.3$ km/s.

2.3 Exercises

Datasets for the exercises are available on *www.issi.unibe.ch/~haaland/Sinaia07/* (or given alternative URL).

1) Estimate the duration of each crossing, and calculate the thickness and orientation of the magnetopause using the 4-SC timing method.

2) Redo the timing analysis with plasma density data. Try to explain any differences in orientation, speed and thickness.

— 3 —

Gradient Methods

An unique property of the Cluster mission is the ability to determine full three dimensional gradients. In this chapter we show how this can be used to determine electric current density from the curlometer technique. Parts of this text is based on Dunlop et al. (1989)

3.1 Theory

Determining the electic current is perhaps the most useful utilization of Cluster's gradient capabilities, but there are also other useful applications, such as checking a vector for divergence, or finding the gradient of a scalar or vector.

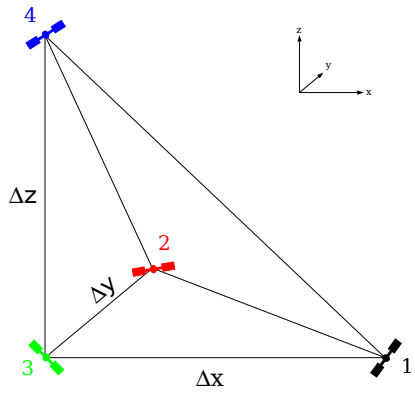

Figure 3.1: *Illustration of the Cluster tetrahedron.*

3.1.1 The curlometer

The curlometer technique utilizes Ampères law and magnetic field :

$$\nabla \times \mathbf{B} = \mu_0 \mathbf{J} \tag{3.1}$$

where $\mathbf{J}$ is the sought after current density. In component form, this is the same as :

$$\begin{aligned} J_x &= \frac{\partial B_y}{\partial z} - \frac{\partial B_z}{\partial y} \\ J_y &= \frac{\partial B_z}{\partial x} - \frac{\partial B_x}{\partial z} \\ J_z &= \frac{\partial B_x}{\partial y} - \frac{\partial B_y}{\partial x} \end{aligned} \tag{3.2}$$

Assuming a linear variation of the field within the spacecraft tetrahedron, Equation 3.3 can be written

$$\begin{aligned} J_x &= \frac{\Delta B_y}{\Delta z} - \frac{\Delta B_z}{\Delta y} \\ J_y &= \frac{\Delta B_z}{\Delta x} - \frac{\Delta B_x}{\Delta z} \\ J_z &= \frac{\Delta B_x}{\Delta y} - \frac{\Delta B_y}{\Delta x} \end{aligned} \tag{3.3}$$

where $\Delta x, \Delta y$ and Δz are determined from the spacecraft separation distance as illustrated in Figure 3.1, and the $\Delta B's$ are the corresponding average change in B-field.

Given the fact that the Cluster tetrahedron is not always of the regular shape illustrated in Figure 3.1, it is often useful to introduce a formalism independent on geometry and coordinate system. This is obtained by concidering the integral form of Ampéres law :

$$\mu_0 \int \mathbf{J} \cdot \mathbf{dS} = \int \mathbf{B} \cdot \mathbf{dl} \tag{3.4}$$

The surface **S** with corners i, j, k (i,j,k=1,2,3,4) in Figure 3.1, is given by :

$$\frac{1}{2} |\Delta \mathbf{R}_{ji} \times \Delta \mathbf{R}_{jk}| \quad i,j,k = 1,2,3,4 \tag{3.5}$$

where $\mathbf{R_{ij}}$ is the spacecraft separation vector betwen spacecraft i and j.

Once again, assuming linear variation of the B-field, the line integral on the right hand side of Equation (3.7), can be expressed :

$$\int \mathbf{B} \cdot \mathbf{dl} = \langle \mathbf{B} \rangle_{ij} \cdot \Delta \mathbf{R}_{ij} + \langle \mathbf{B} \rangle_{ik} \cdot \Delta \mathbf{R}_{ik} + \langle \mathbf{B} \rangle_{jk} \cdot \Delta \mathbf{R}_{jk} \quad i,j,k = 1,2,3,4 \tag{3.6}$$

where the averages, $\langle \mathbf{B} \rangle_{ij} = 1/2(\mathbf{B}_i + \mathbf{B}_j)$. Equation (3.7) can thus be expressed :

$$\mu_0 \mathbf{J} |\Delta \mathbf{R}_{ji} \times \Delta \mathbf{R}_{jk}| = 2 \left(\langle \mathbf{B} \rangle_{ij} \cdot \Delta \mathbf{R}_{ij} + \langle \mathbf{B} \rangle_{ik} \cdot \Delta \mathbf{R}_{ik} + \langle \mathbf{B} \rangle_{jk} \cdot \Delta \mathbf{R}_{jk} \right) \quad i,j,k = 1,2,3,4 \tag{3.7}$$

By using spacecraft 4 as a reference spacecraft, and denoting $\Delta \mathbf{R}_i$ as the relative separation distance for spacecraft i, and $\Delta \mathbf{B}_i$ as the relative magnetic field difference, the above equations can be simplified to :

$$\mu_0 \mathbf{J} \cdot (\Delta \mathbf{R}_i \times \Delta \mathbf{R}_j) = \delta \mathbf{B}_i \cdot \Delta \mathbf{R}_j - \Delta \mathbf{B}_j \cdot \Delta \mathbf{R}_i \quad i,j = 1,2,3 \tag{3.8}$$

where **J** is the average electric current in the tetrahedron.

3.2 Example - determing current density

Since the calculations presented here assume linear variaation of the field within the Cluster tetrahedron, gradient methods usually only work for small spacecraft separation distances. The example event used in the previous chapters had spacecraft separation distances in the order of 1000 km, and thus can not be used to illustrate use of the curlometer.

Figure 3.2 shows an example of the curlometer method to a magnetopause crossing around on 2 March, 2002. During this period, the spacecraft separation was about 100 km, and as seen from the Figure, all four spacecraft are inside the current sheet for a period. The linear approximation should thus be satisfied.

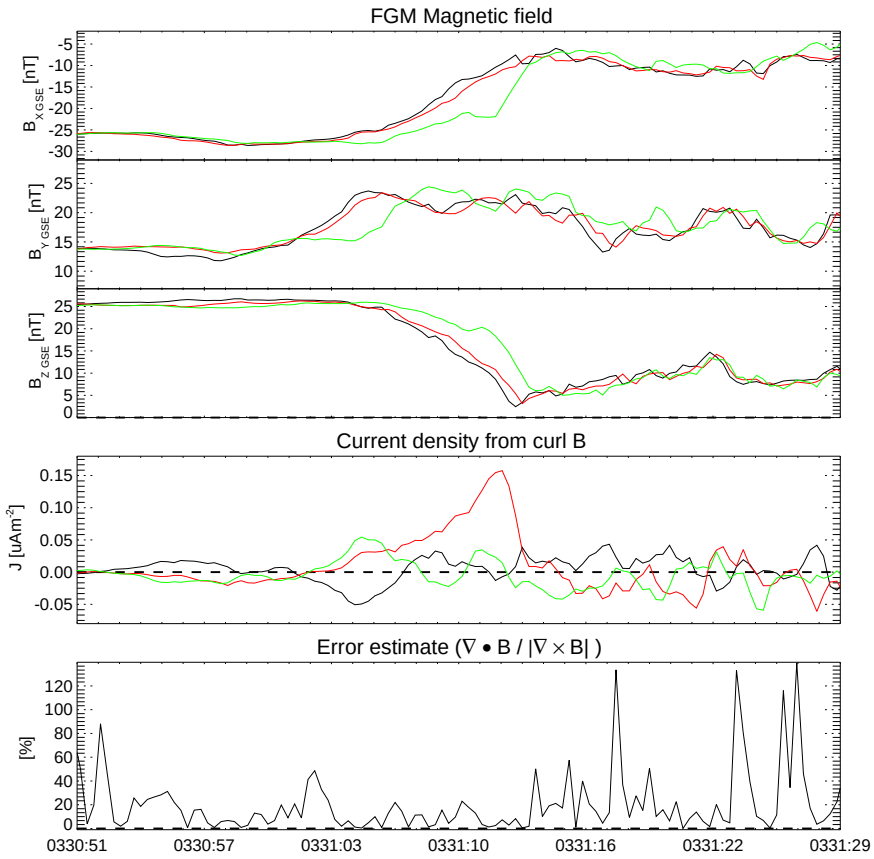

Figure 3.2: *Magnetopause orientation and velocity during a Cluster crossing of the dayside magnetopause around 03:30 UT on 2 March, 2002. Top three panels : Bx, By and Bz GSE components from each spacecraft. Panel 4: Current density Jx (black), Jy (red) and Jz (green) GSE components. Bottom panel Error estimate, here expressed as percentage of* $\nabla \cdot \mathbf{B}/|\nabla \times \mathbf{B}|$.

3.3 Exercises

Datasets for the exercises are available on *www.issi.unibe.ch/∼haaland/Sinaia07* (or given alternative URL).

1) For each spacecraft, perform a minimum variance analysis of the magnetic field in Figure 3.2. Do the orientations obtained differ a lot ?

2) Difficult : Try using the reciprocal vector routines provided earlier and calculate the current (i.e. curl B).

Bibliography

Dunlop, M., D. Southwood, K.-H. Glassmeier, and F. M. Neubauer: 1989, 'Analysis of multipoint magnetometer data'. *Advances in Space research* **8**(9), 273.

Haaland, S., B. Sonnerup, G. Paschmann, E. Georgescu, A. Balogh, B. Klecker, H. Réme, and A. Vaivads: 2006, 'Discontinuity analysis with Cluster'. In: *Proceedings of the Cluster and Double Star Symposium - 5th Anniversary of Cluster in Space*. Nordwiijk: ESA SP-598.

Haaland, S., B. U. Ö. Sonnerup, M. W. Dunlop, A. Balogh, H. Hasegawa, B. Klecker, G. Paschmann, B. Lavraud, I. Dandouras, and H. Rème: 2004, 'Four-Spacecraft Determination of Magnetopause Orientation, Motion and Thickness: Comparison with Results from Single-Spacecraft Methods'. *Annal. Geophysicae* **22**, 1.

Hasegawa, H., B. U. Ö. Sonnerup, M. W. Dunlop, A. Balogh, S. E. Haaland, B. Klecker, G. Paschmann, B. Lavraud, I. Dandouras, and H. Rème: 2004, 'Reconstruction of two-dimensional magnetopause structures from Cluster observations: Verification of method'. *Annal. Geophysicae* **22**.

Khrabrov, A. V. and B. U. Ö. Sonnerup: 1998, 'DeHoffmann-Teller Analysis'. In: G. Paschmann and P. W. Daly (eds.): *Analysis Methods for Multi-Spacecraft Data*, ISSI SR-001. ESA Publications Division, p. 221.

Knetter, T., F. M. Neubauer, T. Horbury, and A. Balogh: 2004, 'Four-point discontinuity observations using Cluster magnetic field data: A statistical survey'. *J. Geophys. Res.* **109**(A18), 6102.

Paschmann, G., S. Haaland, B. U. O. Sonnerup, H. Hasegawa, E. Georgescu, B. Klecker, T. D. Phan, H. Rme, and A. Vaivads: 2005, 'Characteristics of the near-tail dawn magnetopause and boundary layer'. *Annal. Geophysicae* p. 1481.

Sonnerup, B. U. Ö., S. Haaland, G. Paschmann, M. W. Dunlop, H. Rème, and A. Balogh: 2006, 'Orientation and motion of a plasma discontinuity from single-spacecraft measurements: Generic residue analysis of Cluster data'. *Journal of Geophysical Research (Space Physics)* **111**(A10), 5203–5223.

Sonnerup, B. U. O., S. Haaland, G. Paschmann, B. Lavraud, and M. Dunlop: 2004, 'Orientation and Motion of a Discontinuity from Single-spacecraft Measurements of Plasma Velocity and Density: Minimum Massflux Residue'. *J. Geophys. Res.* (A18), 3221.

Sonnerup, B. U. Ö., G. Paschmann, and T. D. Phan: 1995, 'Fluid aspects of reconnection at the magnetopause: in situ observations'. *J. Geophys. Res.*.

Sonnerup, B. U. Ö. and M. Scheible: 1998, 'Minimum and Maximum Variance Analysis'. In: G. Paschmann and P. W. Daly (eds.): *Analysis Methods for Multi-Spacecraft Data*, ISSI SR-001. ESA Publications Division, p. 1850.

Thompson, S. M., M. G. Kivelson, K. K. Khurana, R. L. McPherron, J. M. Weygand, A. Balogh, H. Réme, and L. M. Kistler: 2005, 'Dynamic Harris current sheet thickness from Cluster current density and plasma measurements'. *J. Geophys. Res.* **110**(A9), 2212.